Comparison of RAFT derived Poly(vinylpyrolidone) verses Poly(oligoethyleneglycol methacrylate) for the Stabilization of Glycosylated Gold Nanoparticles

Nga Sze Ieong,[a] Caroline I. Biggs, [a] Mark Walker [a,b] and Matthew I. Gibson [*] [a,c]

a Department of Chemistry, University of Warwick, Gibbet Hill Road, Coventry, CV4 7AL, UK
b Department of Physics, University of Warwick, Gibbet Hill Road, Coventry, CV4 7AL, UK
c Warwick Medical School, University of Warwick, Gibbet Hill Road, Coventry, CV4 7AL, UK
Correspondence to: Matthew I. Gibson (E-mail: *m.i.gibson@warwick.ac.uk)*

(Additional Supporting Information may be found in the online version of this article.)

ABSTRACT: Carbohydrates dictate many biological processes including infection by pathogens. Glycosylated polymers and nanomaterials which have increased affinity due to the cluster glycoside effect, are therefore useful tools to probe function, but also as prophylactic therapies or diagnostic tools. Here, the effect of polymer structure on the coating of gold nanoparticles is studied in the context of grafting density, buffer stability and in a lectin binding assay. RAFT polymerization is used to generate poly(oligoethyleneglycol methacrylates) and poly(*N*-vinyl pyrolidones) with a thiol end-group for subsequent immobilization onto the gold. It is observed that poly(oligoethylene glycol methacrylates), despite being widely used particle coatings, lead to low grafting densities which in turn resulted in lower stability in biological buffers. A depression of the cloud point upon nanoparticle immobilization is also seen, which might compromise performance. In comparison poly(vinyl pyrolidones) resulted in stable particles with higher grafting densities due to the compact size of each monomer unit. The higher grafting density also enabled an increase in the number of carbohydrates which can be installed per nanoparticle at the chain ends, and gave increased binding in a lectin recognition assay. These results will guide the development of new nanoparticle biosensors with enhanced specificity, affinity and stability.

KEYWORDS: Nanoparticle, RAFT Polymerization, Carbohydrate, Lectin, Biosensor

INTRODUCTION Gold nanoparticles (AuNPs) are widely used as biosensors, due to their ease of functionalization with thiolated binding ligands and characteristic optical properties.[1–4] Due to local surface plasmon resonance causing collective oscillations of the conduction-band electrons of the gold core, AuNPs exhibit an intense color in the visible region. The color is strongly correlated with their size, shape, dispersion in media, and degree of aggregation and can thus be used to monitor their interactions. Particles larger than 10 nm and smaller than 100 nm exhibit a red coloration and upon aggregation a dramatic color change, from red to blue, can be observed. Therefore, a suitably functionalized gold nanoparticle will give a color change in the presence of a target which can lead to cross linking,[5] or break an already

formed cross-link.[6] Surface quenched fluorophores can also be released due to ligand binding, generating a fluorescence output.[7] Stevens and coworkers have developed an ultra-sensitive assay format based on gold nanoparticle formation by an amplification route using an enzyme to catalyze silver nucleation around gold nanostars, enabling near single-molecule detection.[8] With any nanoparticle sensor intended for contact with biological fluid it is essential to ensure that it is both colloidally stable to prevent unwanted aggregation and resistant to unwanted protein adhesion (e.g. opsonisation) which both compromise performance.[9] This is typically achieved by the addition of uncharged polymer coatings, which can repel proteins or cells due to their significant surface hydration layer.[10] Messersmith and coworkers used surface-initiated radical polymerization to generate poly(ethylene glycol methacrylate) polymer brushes which could reduce cellular adhesion and spreading[11] although delamination can limit their application.[12] Linear or branched poly(ethylene glycol)s are also widely used as coatings.[13,14] Other commonly employed polymers for this include poly(betaines) and poly(zwitterions).[15] For *in vivo* applications the stability, integrity and ability of the coating to resist opsonisation are crucial to avoid off-specific effects.[16]

One particularly useful method to generate gold-capped nanoparticles is RAFT (reversible additional fragmentation chain transfer) polymerization. In this method, the use of thiocarbonyl compounds results in masked thiols at each chain end, and hence allows facile conjugation onto gold particles (or surfaces) in a fashion similar to self-assembled monolayer formation.[17] A RAFTed polymer can be directly conjugated to small (sub 5 nm) gold nanoparticles by *in situ* reduction with an appropriate gold salt.[18,19] However, to obtain larger nanoparticles, suited to colorimetric detection (typically above 10 nm) preformed gold particles must be used, followed by either grafting-from or grafting-to polymerization.[20] The advantages of grafting-to are that the polymer and nanoparticles can be independently characterized (and, if needed, re-synthesized) to enable fine-tuning of properties, but at the expense of low grafting densities.

Using RAFT polymerization Gibson *et al.* have developed glycan end-functionalized polymers as stabilizing ligands for colorimetric detection of carbohydrate-binding proteins and bacteria.[21,22] This strategy enables the polymer coating to be optimized independent of the glycan (as opposed to having a linear glycopolymer).[23] Using poly(hydroxyethyl acrylamide) as the stabilizing polymer, it was observed that a precise balance must be maintained in the polymer chain length; too long and the particles are too stable so do not aggregate (and hence no color change); too short and they aggregate even without a binding partner, due to low colloidal stability.[24]

In the development of glyconanoparticle sensors such as this, the control of the grafting density is crucial; each polymer chain introduced gives only a single sugar. The affinity of a glycan for its target lectin is inherently weak[25] and is enhanced in nature by presentation of multiple copies, giving rise to a non-linear increase in binding affinity known as the cluster glycoside effect.[26] For example, whilst galactose has a relatively low affinity for the cholera toxin (responsible for the symptoms associated with *Vibreo cholerae* infection) multivalent glycopolymers, glyconanoparticles and glycopeptides have dramatically enhanced binding affinity.[27–29] This strategy has been applied to bind and target many pathogens.[30] Such glyco-materials approaches could help provide innovative solutions to combat the growing problem of antimicrobial resistance

as new biosensors[31] or prophylactic anti-adhesion therapies.[32]

Considering the above, the aim of this work was to critically evaluate the grafting-to of commonly used, water soluble, stabilizing polymers derived from RAFT, for glyconanoparticles. Poly(oligo (ethyleneglycol) methacrylate (OEGMA) which is widely used due to its similarities to linear poly(ethylene glycol). However, it is a rather sterically hindered polymer, especially when compared to a less sterically hindered poly(*N*-vinylpyrolidone), which has been chosen as a model alternative polymer. The role of polymer chain length on the grafting-to efficiency is probed and the stability of the resulting conjugates in a range of relevant media (buffers) is studied. Finally, the utility of these polymers as lectin binding agents is evaluated and rationalized in the context of their grafting-to efficiency.

EXPERIMENTAL

Materials

All reagents and solvents were used as received from the supplier. Laboratory solvents were purchased from Fisher Scientific. Buffer solutions were prepared as follows: phosphate-buffered saline (PBS) solution was prepared by dissolving a pre-formulated tablet (Sigma-Aldrich) in 200 mL ultra-high quality water. The resulting PBS solution has a composition of 0.01 M phosphate, 0.0027 M potassium chloride and 0.138 M sodium chloride, pH 7.4. 10 mmol HEPES (Sigma-Aldrich) buffer, containing 0.1 mmol CaCl2, pH 6.5, was prepared in 250 mL ultra-high quality water. MES buffer (Sigma-Aldrich) was prepared at 100 mmol. S-sec propionic acid O-ethyl xanthate (CTA-1) was synthesized from potassium ethylxanthate and 3-bromopropionic acid (both purchased from Sigma-Aldrich) according to the procedure described in the supplementary information.

Fluorescently labelled lectin (ConA) was purchased from Vector Labs (Fluorescein FLK-2100 labelled). 2-(dodecylthiocarbonothioylthio)-2-methylpropanoic acid (CTA-2), 2-bromopropionic acid, potassium O-ethyl dithiocarbonate, 4,4'-Azobis(4-cyanovaleric acid) and *N*-vinylpyrrolidone, oligo(ethyleneglycol methyl ether methacrylate) were purchased from Sigma-Aldrich. 2-deoxy-2-amino glucose and 2-deoxy-2-amino-galactose were purchased from Carbosynth. Gold nanoparticles were obtained from BBI Solutions. High-binding 96-well microtitre plates were purchased from Greiner Bio-one.

Physical and Analytical Methods

^{1}H and ^{13}C NMR spectra were recorded on Bruker DPX-300 and DPX-400 spectrometers using deuterated solvents obtained from Sigma-Aldrich. Chemical shifts are reported relative to residual non-deuterated solvent. Size exclusion chromatography (SEC) was used to determine the molecular weights and polydispersities of the synthesised polymers. The THF SEC system comprised of a Varian 390-LC-Multi detector suite fitted with differential refractive index (DRI), light scattering (LS) and ultra-violet (UV) detectors equipped with a guard column (Varian Polymer Laboaratories PLGel 5µm, 50 x 7.5mm) and two mixed D columns of the same type. The mobile phase was THF with 5% triethylamine (TEA) eluent at a flow of 1.0 mL.min^{-1}, and samples were calibrated against Varian Polymer Laboratories Easi Vials linear poly(styrene) and poly(methylmethacrylate) standards (162-2.4 x 105 g.mol^{-1}) using Cirrus v3.3. The DMF SEC system comprised of a Varian 390-LC-Multi detector suite fitted with a differential refractive index (DRI) detector equipped with a guard column (Varian Polymer

Laboaratories PLGel 5µm, 50 x 7.5 mm) and two mixed D columns of the same type. The mobile phase was DMF with 5 nM NH3BF4 eluent at a flow of 1.0 mL.min^{-1}, and samples were calibrated against Varian Polymer Laboratories Easi-Vials poly(methylmethacrylate) standards (162-2.4 x 105 g.mol^{-1}) using Cirrus v3.3.

Synthesis of PVP_X (X = 80, 110, 250) using S-sec propionic acid O-ethyl xanthate RAFT agent (CTA-1)

As a representative example *N*-vinylpyrrolidone (VP) (1.00 g, 0.009 mol), CTA-1 (8.7 mg, 0.045 mmol) and ACVA (0.273 mL of 4.62 mg.mL^{-1} dioxane) were dissolved in 1,4-dioxane (1 mL) in a vial. The resulting solution was purged with a stream of dry nitrogen for 15 min and then heated at 80 °C for 7 h after which an aliquot was taken from the mixture for ^{1}H NMR conversion analysis. Conversions were calculated using ^{1}H NMR spectroscopy by comparing the integrations of the heterocycle signals on the VP monomer (δ=3.49 ppm) with those of the corresponding signals of the polymer (δ=3.20 ppm). The colourless solution was then quenched with ice. The crude mixture was concentrated in vacuo, diluted with nanopure water, and dialyzed against nanopure water (MWCO = 1 kDa) to remove any unreacted VP and small molecule byproducts. Poly(*N*-vinylpyrrolidone) (PVP_{60}) was recovered as an off-white powder (0.3 g, ca. 71 % based on 42 % conversion) after being freeze-dried. ^{1}H NMR (400 MHz, $CDCl_3$): δ=3.79 (-NCH, br, ^{1}H), 3.20 (-NCH_2-, br, 2H), 2.70-0.88 (O=C-CH_2-, -CH_2- on heterocycle, -CH_2- on polymer backbone, br, 6H). MnSEC(DMF) = 7.2 kDa, Mw/Mn = 1.46.

***Synthesis of $POEGMA_X$ (X = 70, 120, 230) using RAFT agent (*CTA-2)**

As a representative example, oligo(ethyleneglycol methyl ether methacrylate) (OEGMA) (1.00 g, 0.0033 mol), CTA-2 (12.1 mg, 0.033 mmol) and ACVA (1.01 uL of 1.85 mg.mL^{-1} dioxane) were dissolved in 1,4-dioxane (3 mL) in a vial. The resulting solution was purged with a stream of dry nitrogen for 15 min and then heated at 70 °C for 4 h after which an aliquot was taken from the mixture for ^{1}H NMR conversion analysis. Conversions were calculated using ^{1}H NMR spectroscopy by comparing the integrations of the -C=O(O)CH_2- signals on the OEGMA monomer (δ= 4.30 ppm) with those of the corresponding signals of the polymer side chain (δ= 4.03 ppm). The colourless solution was then quenched with ice. The crude mixture was then precipitated from methanol into diethylether three times until - residual monomer and small molecules were undetectable by ^{1}H NMR spectroscopy. Poly(oligo(ethyleneglycol methyl ether methacrylate)) ($POEGMA_{70}$) was recovered as a yellow waxy solid (0.5 g, ca. 74 % based on 68 % conversion). ^{1}H NMR (400 MHz, $CDCl_3$): δ= 4.03 (-C=O(O)CH_2H_2-, br, 2H), 3.61 (-OCH_2-, br, 16H), 3.51 (-C=O(O)CCH_2H_2-, br, 2H), 3.33 (-OCH_3, br, 3H), 2.13-1.52 (-CH_2- on polymer backbone, br, 2H), 1.31-0.59 (-$CHCH_3$- on polymer backbone, br, 3H). MnSEC(THF) = 56 kDa, Mw/Mn = 1.51.

General procedure for the synthesis of polymer-coated gold nanoparticles

A solution of gold nanoparticles (40 nm, 40 mL) was added to a falcon tube. The desired polymer (ca. 8 mg) was then added to the above red solution which was then agitated until all the polymer was dissolved. The resulting solution was then allowed to stand at ambient conditions in the dark overnight. To remove excess polymer, the particles were centrifuged for 15 min at 11000 rpm. The colourless supernatant was decanted and the pellet was then resuspended in nanopure water (10 mL). This centrifugation-

resuspension cycle was then repeated for two more times. After the final cycle the particles were dispersed in 10 mL of MES buffer (0.1 M) for storage or the desired buffer (PBS, HEPES, nanopure water) for further studies. Assuming complete transformation of naked gold particles into the polymer-coated particles, the total concentration of gold in the final solution was 0.2332 $mg.mL^{-1}$.

RESULTS AND DISCUSSION

To enable a critical comparison to be made between the commonly employed oligo(ethyleneglycol)methacrylate (OEGMA) based polymers and a less sterically hindered, water-soluble alterative (*N*-vinylpyrolidone) (PVP), RAFT/MADIX polymerization was employed. This method enables the synthesis of well-defined polymers with masked thiol end groups to enable direct conjugation onto citrate-stabilized gold nanoparticles, Scheme 1. Following RAFT polymerization, the degree of conversion for each polymer was estimated by ^{1}H NMR (assuming quantitative incorporation of the RAFT mediating agent). SEC of PVP is well known to underestimate its molecular weight, due to poor solvation (accept in fluorinated solvents which are very rarely employed),[33] which also means that observed dispersity values are above what might be expected from RAFT. The same is true for the POEGMAs, whose comb-like structure results in hydrodynamic radii that are significantly different from linear polymers. In all cases monomodal distributions were obtained. The results of these analyses are shown in Table 1 and example SEC traces shown in Figure 1, showing the sequential library of polymers ranging from 70 to 250 repeat units.

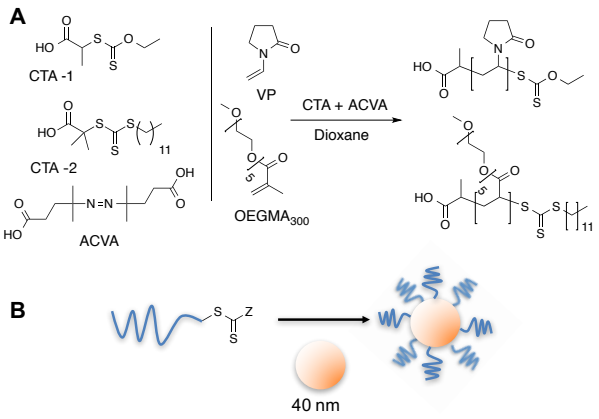

SCHEME 1 (A) Synthesis of polymers. CTA = chain transfer (RAFT) agent; ACVA = 4,4-Azobis(4-cyanopentanoic acid); VP = *N*-vinylpyrolidone; (B) Assembly of polymers onto pre-formed gold nanoparticles.

TABLE 1 RAFT synthesized polymers

Code	Con.[(a)] (%)	DP [a]	$M_{n\ (theo.)}$ (kDa)[a]	$M_{n\ (SEC)}$ (kDa)	M_w/M_n
PVP_{80}	42	84	10.9	7.2 [b]	1.46[b]
PVP_{110}	37	111	12.3	10.4 [b]	1.51[b]
PVP_{250}	58	247	27.4	19.0 [b]	1.75[b]
$POEGMA_{70}$	68	68	20.4	56.0 [c]	1.51[c]
$POEGMA_{120}$	57	114	34.2	74.9 [c]	1.57 [c]
$POEGMA_{230}$	59	236	70.8	134.0 [c]	1.53 [c]

[a] Determined from the [monomer]:[CTA] ratio and the degree of polymerization (DP). [b] Determined by SEC in DMF using PMMA standards. [c] Determined by SEC in THF using PMMA standards.

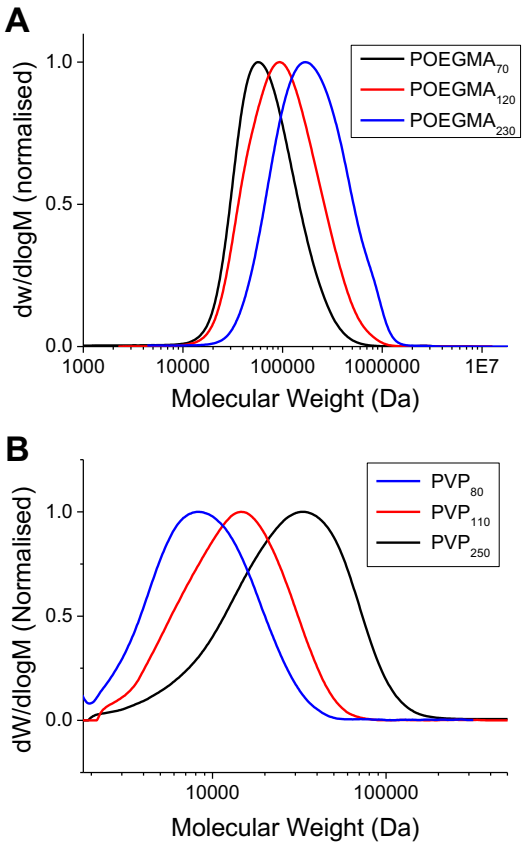

FIGURE 1 SEC analysis of RAFT-derived polymers. SEC was conducted in DMF and molecular weights calculated relative to PMMA standards. (A) POEGMA; (B) PVP.

With these polymers to hand, they were employed to coat citrate-stabilized 40 nm gold nanoparticles (Au_{40}). Surface modification of the particles was achieved by a simple mixing protocol using an excess of the polymer overnight with the exclusion of light. Purification was achieved by repeated centrifugation/resuspension cycles to remove excess polymer and the isolated nanoparticles had a burgundy-red coloration in aqueous solution, indicative of no aggregation. Dynamic light scattering analysis revealed the obtained particles had increased diameters ranging from 55–90 nm, compared to the precursor particles, as shown in Figure 2. The longer polymers (DP >200) gave slightly larger (~ 10 nm) hydrodynamic diameters relative to the shorter ones, as would be expected.

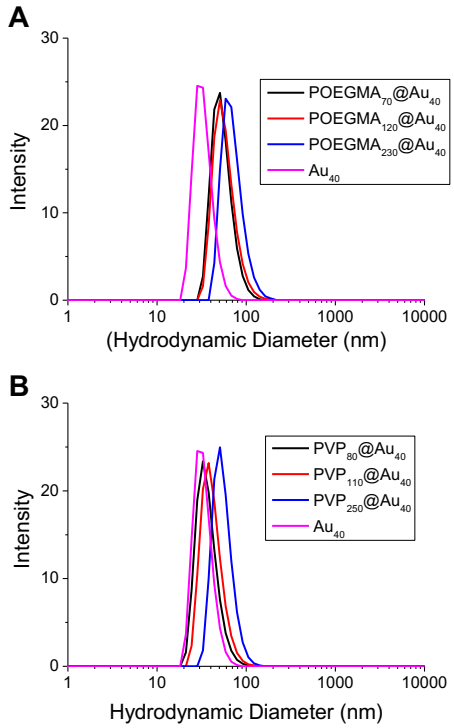

FIGURE 2 Dynamic light scattering analysis of polymer-coated gold nanoparticles. (A) POEGMA-coated nanoparticles; (B) PVP-coated nanoparticles.

The ultimate application of these functionalized nanoparticles is to incorporate glycans at the polymer's corona for biosensory applications, meaning that the grafting density (number of chains per unit area) on surfaces is a key parameter in defining their properties.[31,34,24] This is especially important in the case of end-functionalized polymer-coatings where ligands (such as sugars or drugs) are incorporated at the chain end, as the grafting density is directly proportional to the loading capacity. To estimate the relative grafting density (rather than the absolute) in this series, X-ray photoelectron spectroscopy (XPS) was performed. It is important to note that the penetration depth of the X-rays is estimated to be ~ 10 nm, so it can only be used to measure the relative grafting density.

As all the particles have identical gold cores (and hence equal gold surface 'concentration') one can estimate the grafting density, from the relative elemental compositions and MW information, according to Equation 1. Samples were prepared by deposition of the particles from solution onto silicon surfaces and the results are shown in Figure 3.

$$G.D = Ic \,/\, (Number\ Carbons\ in\ Monomer \times DP)$$

Equation 1 G.D = relative grafting density; I^C = intensity of carbon signals after normalization to gold signal.

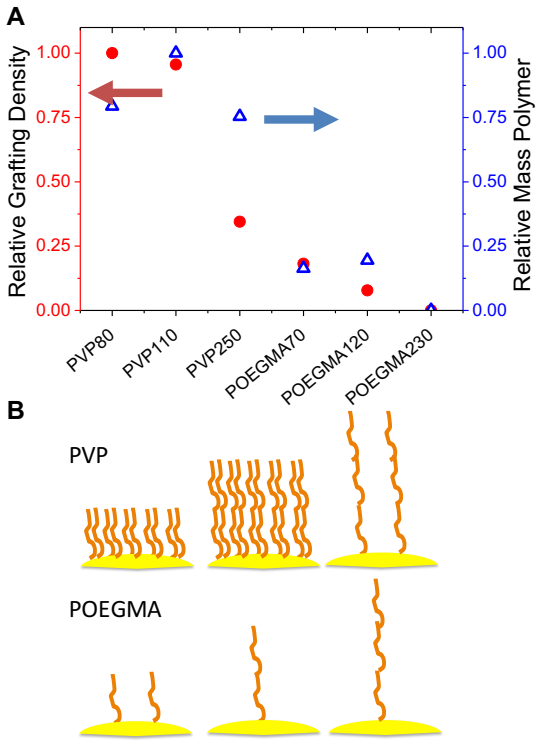

FIGURE 3 Grafting density comparison as estimated by XPS analysis. (A) Comparison of relative (assuming PVP_{80} = 1) grafting density (chains/unit area) and overall mass of polymer; (B) Schematic comparing relative grafting densities as a function of chain length and monomer type.

As the PVP chain length increased from 80 to 110 there was no appreciable difference in the grafting density, but once it was increased to DP 250, the grafting density decreased to only 25 % of that of DP 80. This shift in grafting density will be due to the increased steric requirements of the polymer, but one must also remember that at equal mass concentration, there are less end-groups available for larger polymers which may also have an influence (although in our case a huge excess of polymer is employed). When PVP is compared to POEGMA, it is found that POEGMA has significantly fewer chains immobilized onto the surface. $POEGMA_{70}$ (shortest polymer used in this study) had 25 % of the polymer chains compared to a similar length PVP, and less total mass also. The longer POEGMAs also had lower grafting densities, and they are summarized in Figure 3B. These findings are remarkable considering the wide spread use of POEGMA as a stabilizing agent, and implies that it might not provide as efficient a steric shield as other 'non-fouling' polymers.

The above experiments clearly demonstrated that the steric constraints of the polymer side chain affect grafting density, but this information is only useful in the context of observable properties of the resulting particles. For biosensory applications nanoparticles must be stable against aggregation,[35] hence this was studied in a range of conditions. Due to the well-known SPR properties of gold nanoparticles, it is possible to evaluate aggregation spectrophotometrically by observing the changes in the UV-Vis spectra of the particles as they change from dispersed (red) to aggregated (blue), Figure 4A and B. A high-throughput method using 96-plates and microplate readers was employed to evaluate stability in saline solutions from 0.5 - 2 M and in MES and PBS; two common buffers. The absorbance at 520 nm reflects the

aggregation state (with high values meaning well dispersed particles), and the results are shown in Figure 4C and 4D as a function of the media after 1 hour incubation at 37 °C. All the polymers with DP 70 showed little evidence of aggregation in saline, and the PVP polymers with DP > 100 were perfectly dispersed even up to 2 M NaCl, which is far above physiological concentrations (~ 0.14 M). Conversely, the POGEMA –coated particles aggregated to some degree in all NaCl concentrations. A similar observation was made in all buffers apart from PBS, in which limited aggregation was seen for all the particles employed. This aggregation will be a combination of the lower grafting density of the polymer brushes, but could also be due to the OEG side chains coordinating metal salts, depressing the LCST and hence leading to aggregation.[36] This simple test shows that POEGMA particles may not be suitable in colorimetric bioassays as their premature aggregation would give rise to false positive results, which are not acceptable for diagnostics.

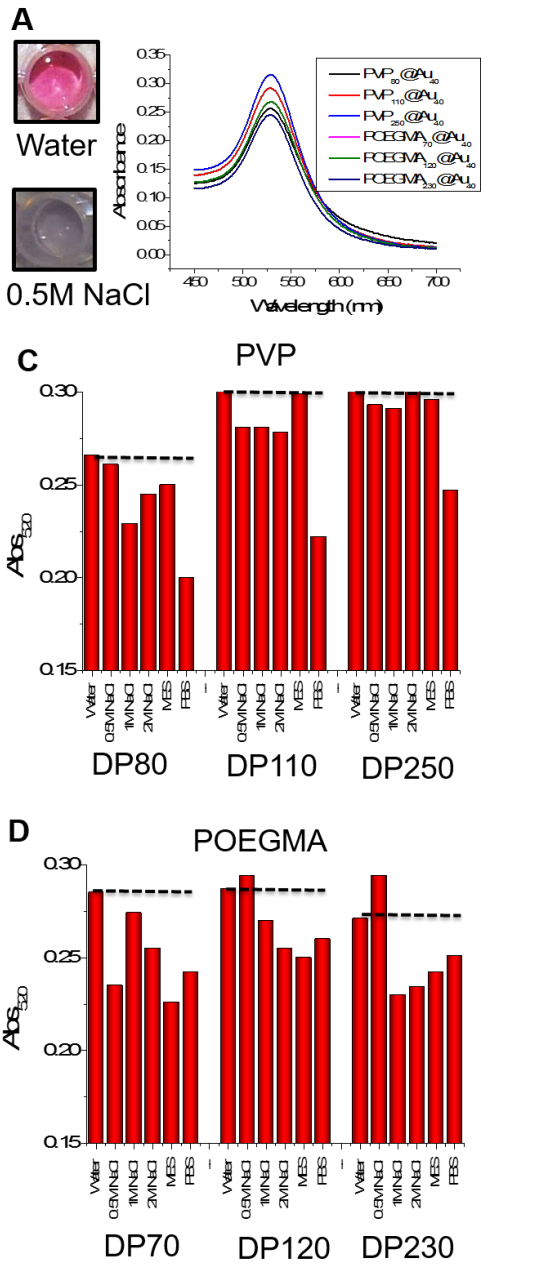

FIGURE 4 Saline stability testing of the nanoparticles. (A) Photographs showing the effect of addition of salt on citrate-coated AuNPs, demonstrating the red-blue color change due to aggregation of AuNPs; (B) Spectrophotometric analysis showing the absorbance of each differently coated nanoparticle; (C) and (D) Absorbance of each nanoparticle at 520 nm in each of the six solutions.

A second problem with using POEGMAs is that they show LCST (soluble to insoluble transition above a critical temperature) behavior that may lead to aggregation if an assay was run at temperatures close to this transition temperature. This is an issue, even if the polymers themselves have high LCSTs, as we have previously shown that immobilization onto nanoparticle surfaces decreases the transition temperature, relative to free polymers in solution.[37,38,39] The polymer library (Table 1) was assessed for LCST behavior by turbidimetry at 5 mg.mL^{-1} in both water and PBS, and the traces are shown in Figure 5. The POEGMAs all showed cloud points (CPs) around 55 °C, whereas the PVP showed no transition up to 90 °C. It should be noted that at higher concentrations, the PVP would be expected to show a CP but these are far beyond what would be employed in this situation.

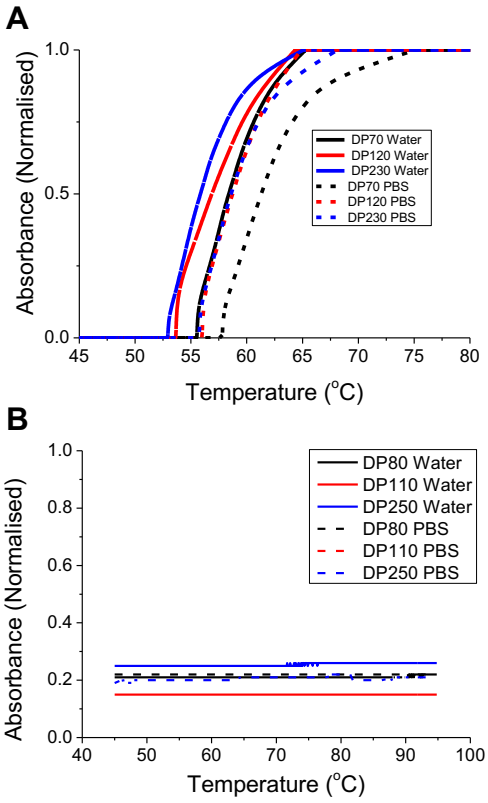

FIGURE 5 Turbidimetry analysis of polymers in Table 1. All measurements were conducted in water or PBS at 3 mg.mL^{-1}. (A) POEGMA; (B) PVP.

The polymer-coated nanoparticles were also investigated for their LCST behavior. Full temperature-dependent UV-Vis spectra for each of the nanoparticles are included in Figure 6. For all the PVP samples, increasing the temperature from 35 to 85 °C resulted in no observable changes in the absorption spectra, indicating the nanoparticles are perfectly stable. Conversely, heating the POEGMA-coated nanoparticles resulted in a clear decrease in SPR_{max}, and increase in Abs_{700} upon heating above 50 °C. Whilst above the most likely assay temperatures of 37 °C, the transition temperature is known to decrease sharply upon addition of higher salt concentrations. This effect is also observed with other additives, such as sugars or proteins, which are present in biological milieu. Hence, the POEGMA particles have potential for premature aggregation due to this LCST effect as well as salting out in buffers, as discussed above.

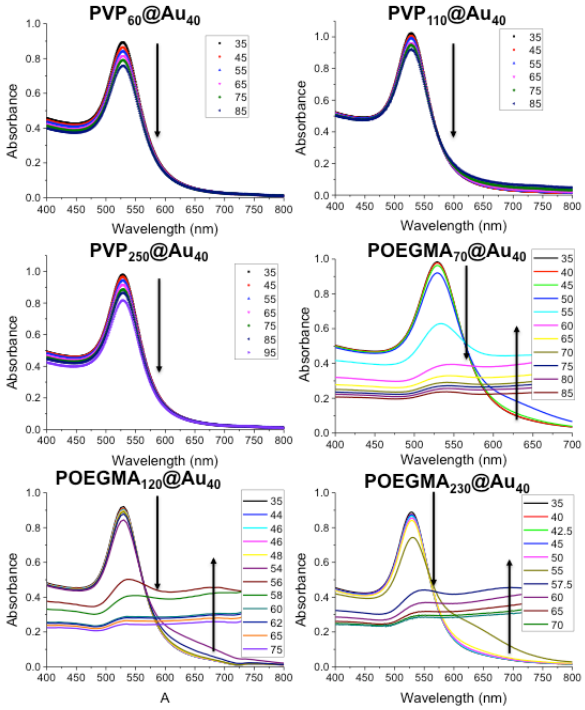

Figure 6 Assessment of the LCST behavior of polymer-coated gold nanoparticles. All

measurements were conducted in PBS. Arrows indicate changes in spectral features and are intended to guide the eye only.

With this detailed understanding of the particle properties to hand, the final step was to conduct lectin binding experiments to compare the influence of grafting density and polymer structure on a real outcome. The RAFT agents used to synthesize the polymers were chosen to introduce a carboxylic acid group at its α-terminus, which is available for bioconjugation. 2-deoxy-2-amino glucose ($GlcNH_2$) and 2-deoxy-2-amino-galactose ($GalNH_2$) were chosen as biological binding motifs that can be introduced by simple EDC/NHS activation of the carboxylic acid, Figure 7A. Following removal of excess carbohydrate and coupling reagents by centrifugation/resuspension, the biological activity of the particles was tested by a modified surface-binding assay. In brief, high-binding 96-well plates were coated with concanavalin A (ConA), a lectin which has higher binding affinity to glucose than galactose (with an ultimate preference for α-mannose). The particles were incubated with these surfaces at 37 °C for 30 minutes in HEPES buffer (containing Ca^{2+}), before being extensively washed to remove any non-specifically bound particles. The relative affinity of the interaction was determined by measuring the absorbance at 520 nm (gold particle SPR band) on the plates, which is proportional to the amount of gold particles bound. PVP_{250} with both galactose and glucose end-groups showed essentially no particle interactions even at concentrations as high as 0.2 $mg.mL^{-1}$ [Au], Figure 7. Conversely, the shorter PVP (DP = 110) which was found to have a grafting density 4 x as high as the longer polymer (but identical saline stability), showed a clear dose dependence increase in surface binding of the glucose-functional particles, which was significantly higher than the corresponding galactose particles (which also have weak ConA affinity). All POEGMAs showed some signs of aggregation in the binding buffer, preventing analysis. Taken together, these observations show that designing glyconanoparticles for biological applications requires substantial consideration of the nature of the polymer layer, which should not be over-simplified as a passive, non-interacting layer, but actually as a key component which needs refinement for each application. These observations made here will help guide ourselves, and others, in the design of point-of-care diagnostics or drug delivery devices which employ carbohydrates.

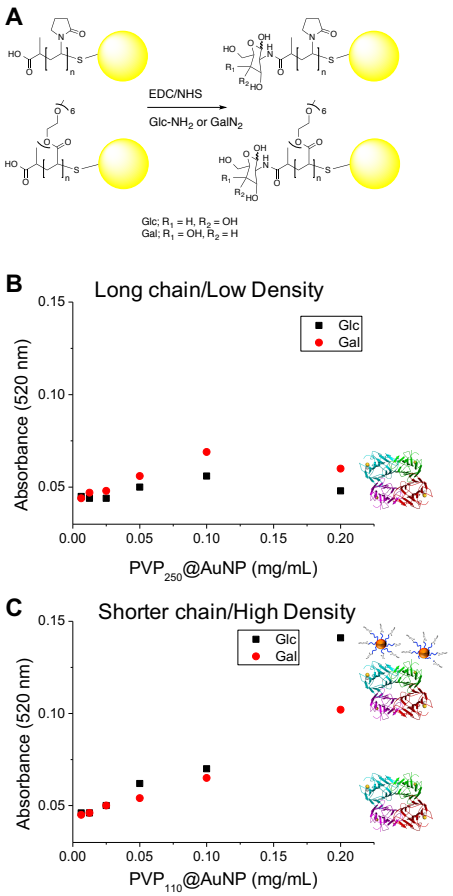

FIGURE 7 (A) Conjugation of amino-glycosides to carboxylic-acid terminated, polymer-coated nanoparticles; Binding assays to ConA surfaces using (B) PVP_{250}

(long) with little particle binding; (C) PVP_{110} (short) showing stronger binding of Con A to the polymer coated AuNPs.

CONCLUSIONS

Here a library of polymer-stabilized gold nanoparticles were synthesized, characterized and critically evaluated for their utility in biosensing. Two commonly employed classes of water soluble polymer were used, POEGMA and PVP, as these are both neutral and are non-fouling towards non-specific protein adhesion. Using XPS it was shown that the sterically bulky POEGMA resulted in far lower grafting densities on gold nanoparticles compared to PVP, suggesting a greater degree of exposed gold surfaces. Colloidal stability assays were undertaken, using the aggregation-induced red-blue color change of gold nanoparticles as the output. This showed that the PVP colloids were more stable, attributable to their greater surface coverage. The impact of surface-grafting on the LCST behavior of the particles was also measured, and it was shown that in the case of longer POEGMAs, aggregation occurred at temperatures close to what might be used in a biosensor. Finally, the polymers were glycosylated at their end-group and evaluated for binding to a surface-bound lectin. Owing to the higher grafting density (at equal degree of polymerization) the PVP polymers resulting in more surface binding. Taken together, this study shows that sterically bulky POEGMAs are not suitable stabilizing agents for gold nanoparticles obtained by 'grafting-to' and that small, sterically less hindered poly(acrylamides) give higher grafting densities and hence more ligand attachment. These results will help in the rationale designed of new biosensors, especially glycobiosenors for infection.

ACKNOWLEDGEMENTS

Equipment used was supported by the Birmingham Science City (SC) Advanced Materials project, with support from Advantage West Midlands and part funded by the European Regional Development Fund. MIG holds an ERC starting grant (CRYOMAT 638661). CIB held a PhD Scholarship from the BBSRC-funded Life Science Training Centre.

REFERENCES

1 K. Saha, S. S. Agasti, C. Kim, X. Li and V. M. Rotello, *Chem. Rev.* **2012**, *112*, 2739–2779.
2 X. Cao, Y. Ye and S. Liu, *Anal. Biochem.,* **2011**, *417*, 1–16.
3 C. J. Murphy, A. M. Gole, J. W. Stone, P. N. Sisco, A. M. Alkilany, E. C. Goldsmith and S. C. Baxter, *Acc. Chem. Res.*, **2008**, *41*, 1721–1730.
4 P. K. Jain, X. Huang, I. H. El-Sayed and M. A. El-Sayed, *Plasmonics*, **2007**, *2*, 107–118.
5 R. Elghanian, J. J. Storhoff, R. C. Mucic, R. L. Letsinger and C. A. Mirkin, *Science*, **1997**, *277*, 1078–1081.
6 A. Laromaine, L. Koh, M. Murugesan, R. V. Ulijn and M. M. Stevens, *J. Am. Chem. Soc.*, **2007**, *129*, 4156–4157.
7 C.-C. You, O. R. Miranda, B. Gider, P. S. Ghosh, I.-B. Kim, B. Erdogan, S. A. Krovi, U. H. F. Bunz and V. M. Rotello, *Nat. Nanotechnol.*, **2007**, *2*, 318–323.
8 L. Rodríguez-Lorenzo, R. de la Rica, R. A. Álvarez-Puebla, L. M. Liz-Marzán and M. M. Stevens, *Nat Mater.*, **2012**, *11*, 604–607.
9 M. Lundqvist, J. Stigler, G. Elia, I. Lynch, T. Cedervall and K. A. Dawson, *Proc. Natl. Acad. Sci. U. S. A.*, **2008**, *105*, 14265–70.
10 S. Chen, L. Li, C. Zhao and J. Zheng, *Polymer*, **2010**, *51*, 5283–5293.
11 X. Fan, L. Lin and P. B. Messersmith, *Biomacromolecules*, **2006**, *7*, 2443–2448.
12 S. Tugulu and H. A. Klok, *Biomacromolecules*, **2008**, *9*, 906–912.
13 J. Groll, Z. Ademovic, T. Ameringer, D.

Klee and M. Moeller, *Biomacromolecules*, **2005**, *6*, 956–962.
14 M. Binazadeh, M. Kabiri and L. D. Unsworth, in *ACS Symposium Series*, **2012**, vol. 1120, pp. 621–643.
15 A. M. Alswieleh, N. Cheng, I. Canton, B. Ustbas, X. Xue, V. Ladmiral, S. Xia, R. E. Ducker, O. El Zubir, M. L. Cartron, C. N. Hunter, G. J. Leggett and S. P. Armes, *J. Am. Chem. Soc.*, **2014**, *136*, 9404–9413.
16 W. G. Kreyling, A. M. Abdelmonem, Z. Ali, F. Alves, M. Geiser, N. Haberl, R. Hartmann, S. Hirn, D. J. de Aberasturi, K. Kantner, G. Khadem-Saba, J.-M. Montenegro, J. Rejman, T. Rojo, I. R. de Larramendi, R. Ufartes, A. Wenk and W. J. Parak, *Nat. Nanotechnol.*, **2015**, *10*, 619–23.
17 J. C. Love, L. A. Estroff, J. K. Kriebel, R. G. Nuzzo and G. M. Whitesides, *Chem. Rev.*, **2005**, *105*, 1103–1170.
18 A. B. Lowe, B. S. Sumerlin, M. S. Donovan and C. L. McCormick, *J. Am. Chem. Soc.*, **2002**, *124*, 11562–11563.
19 S. G. Spain, L. Albertin and N. R. Cameron, *Chem. Commun.*, **2006**, *96,* 4198–200.
20 R. Barbey, L. Lavanant, D. Paripovic, N. Schuwer, C. Sugnaux, S. Tugulu and H.-A. Klok, *Chem. Rev.*, **2009**, *109*, 5437–5527.
21 L. Otten, E. Fullam and M. I. Gibson, *Mol. Biosyst.*, **2016**, *12*, 341–344.
22 L. Otten, S.-J. Richards, E. Fullam, G. S. Besra and M. I. Gibson, *J. Mater. Chem. B*, **2013**, *1*, 2665–2672.
23 J. Lu, W. Zhang, S.-J. Richards, M. I. Gibson and G. Chen, *Polym. Chem.*, **2014**, *5*, 2326–2332.
24 S.-J. Richards and M. I. Gibson, *ACS Macro Lett.*, **2014**, *3*, 1004–1008.
25 M. Ambrosi, N. R. Cameron and B. G. Davis, *Org. Biomol. Chem.*, **2005**, *3*, 1593–608.
26 J. J. Lundquist and E. J. Toone, *Chem. Rev.*, **2002**, *102*, 555–578.
27 S.-J. Richards, M. W. Jones, M. Hunaban, D. M. Haddleton and M. I. Gibson, *Angew. Chemie - Int. Ed.*, **2012**, *51*, 7812–7816.
28 M. W. Jones, L. Otten, S.-J. Richards, R. Lowery, D. J. Phillips, D. M. Haddleton and M. I. Gibson, *Chem. Sci.*, **2014**, *5*, 1611–1616.
29 T. R. Branson, T. E. McAllister, J. Garcia-Hartjes, M. A. Fascione, J. F. Ross, S. L. Warriner, T. Wennekes, H. Zuilhof and W. B. Turnbull, *Angew. Chemie - Int. Ed.*, **2014**, *53*, 8323–8327.
30 T. R. Branson and W. B. Turnbull, *Chem. Soc. Rev.*, **2013**, *42*, 4613–22.
31 L. Otten, D. Vlachou, S.-J. Richards and M. I. Gibson, *Analyst*, **2016**, *141*, 4305–4312.
32 N. Sharon, *Biochim. Biophys. Acta - Gen. Subj.*, **2006**, *1760*, 527–537.
33 N. S. Ieong, M. Hasan, D. J. Phillips, Y. Saaka, R. K. O'Reilly and M. I. Gibson, *Polym. Chem.*, **2012**, *3*, 794–799.
34 S.-J. Richards, C. I. Biggs and M. I. Gibson, *Multivalent glycopolymer-coated gold nanoparticles*, **2016**, vol. 1367.
35 M. I. Gibson, M. Danial and H.-A. Klok, *ACS Comb. Sci.*, **2011**, *13*, 286–297.
36 J. P. Magnusson, A. Khan, G. Pasparakis, A. O. Saeed, W. Wang and C. Alexander, *J. Am. Chem. Soc.*, **2008**, *130*, 10852–10853.
37 H.-A. Klok, M. I. Gibson and D. Paripovic, *Adv. Mater.*, **2010**, *22*, 4721–4725.
38 N. S. Ieong, K. Brebis, L. E. Daniel, R. K. O'Reilly and M. I. Gibson, *Chem. Commun.*, **2011**, *47*, 11627–11629.
39 S. Won, D. J. Phillips, M. Walker and M. I. Gibson, *J. Mater. Chem. B*, **2016**, *118*, 1634.

GRAPHICAL ABSTRACT

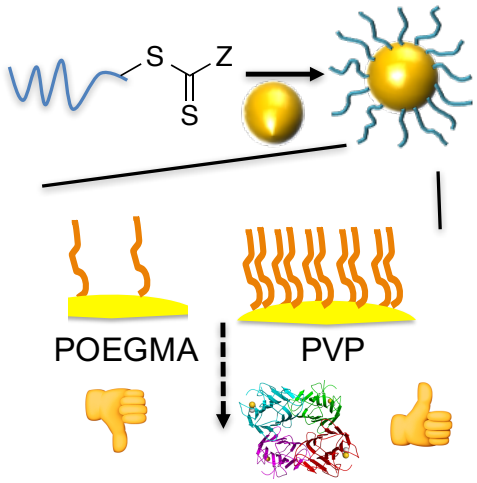

Nga Sze Ieong,[a] Caroline I. Biggs,[a] Mark Walker[a,b] and Matthew I. Gibson*[a,c]

Comparison of RAFT derived Poly(vinylpyrolidone) verses Poly(oligoethyleneglycol methacrylate) for the Stabilization of Glycosylated Gold Nanoparticles

TEXT ((up to 75 words, not the same as the abstract text, present tense, no personal pronouns, written for a non-specialist, see recent issue for examples))

A critical comparison is made between a commonly used comb-shaped polymer (POEGMA) and linear polymer (PVP) for their stabilization of gold nanoparticles for biosensing. It is shown that the PVP gives rise to higher grafting densities and improved saline stability. Furthermore, introduction of carbohydrates at the polymer end-group resulted in more binding to a model lectin for the PVP system compared to POEGMA. This highlights the crucial role of the polymer corona for plasmonic nanosensors.